Science of the Total Environment 877 (2023) 162947

Contents lists available at ScienceDirect

Science of the Total Environment

journal homepage: www.elsevier.com/locate/scitotenv

Atmospheric deposition of microplastics in a rural region of North China Plain

Jingjing Li [a,b,1], Jinrui Zhang [a,b,1], Siyang Ren [a,c], Daqi Huang [d], Fobang Liu [e], Zhen Li [f], Hanyue Zhang [a,g], Mingyu Zhao [a,b], Yuxuan Cao [a,b], Samson Mofolo [a,b], Jiexi Liang [a], Wen Xu [a,b], Davey L. Jones [c,h], David R. Chadwick [c], Xuejun Liu [a,b], Kai Wang [a,b,*]

[a] College of Resources and Environmental Sciences, National Academy of Agriculture Green Development, Key Laboratory of Plant-Soil Interactions of Ministry of Education, Beijing Key Laboratory of Farmland Soil Pollution Prevention and Remediation, China Agricultural University, Beijing 100193, PR China
[b] National Observation and Research Station of Agriculture Green Development (Quzhou, Hebei), China Agricultural University, Beijing 100193, PR China
[c] School of Natural Sciences, Bangor University, Bangor, Gwynedd LL57 2UW, UK
[d] Shenyuan Honors College, Beihang University, Beijing 100191, PR China
[e] Department of Environmental Science and Engineering, Xi'an Jiaotong University, Xi'an, Shaanxi 710049, PR China
[f] Institute of Environment and Sustainable Development in Agriculture, Chinese Academy of Agricultural Sciences, Beijing 100081, PR China
[g] Soil Physics and Land Management Group, Wageningen University & Research, Wageningen 6700 AA, the Netherlands
[h] SoilsWest, Centre for Sustainable Farming Systems, Food Futures Institute, Murdoch University, Murdoch, WA 6150, Australia

HIGHLIGHTS

- Microplastic in atmospheric bulk deposition in a rural region, NCP was detected.
- Atmospheric microplastic number was 1–2 order of magnitude higher than other study.
- Positive correlation between atmospheric microplastic and rainfall was observed.
- Source of atmospheric microplastic was analyzed by HYSPLIT back-trajectory model.

GRAPHICAL ABSTRACT

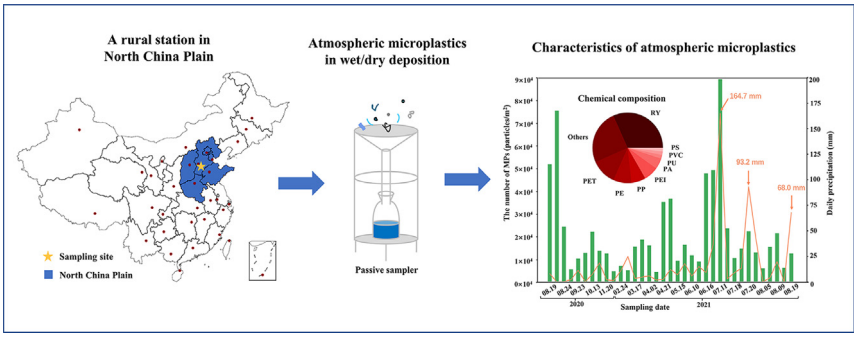

ARTICLE INFO

Editor: Thomas Kevin V

Keywords:
Atmospheric microplastics
Particle number and size
Chemical composition
Seasonal variation
Transport modelling
Rural region

ABSTRACT

Microplastics (MPs) pollution is becoming one of the most pressing environmental issues globally. MPs in the marine, freshwater and terrestrial environments have been fairly well investigated. However, knowledge of the atmospheric-mediated deposition of MPs within rural environments is limited. Here, we present the results of bulk (dry and wet) atmospheric MPs deposition in a rural region of Quzhou County in the North China Plain (NCP). Samples of MPs in the atmospheric bulk deposition were collected for individual rainfall events over a 12-month period from August 2020 to August 2021. The number and size of MPs from 35 rainfall samples were measured by fluorescence microscopy, while the chemical composition of MPs was identified using micro-Fourier transform infrared spectroscopy (μ-FTIR). The results showed that the atmospheric MPs deposition rate in summer (892–75,421 particles/m^2/day) was highest compared to 735–9428, 280–4244 and 86–1347 particles/m^2/day in spring, autumn, and winter, respectively. Furthermore, the MPs deposition rates in our study were 1–2 orders of magnitude higher than those in other regions, indicating a higher rate of MPs deposition in the rural region of the NCP. MPs with a diameter of 3–50 μm accounted for 75.6 %, 78.4 %, 73.4 % and 66.1 % of total MPs deposition in spring, summer, autumn, and winter, respectively, showing that the majority of MPs in the current study were small in size. Rayon fibers accounted for the largest

* Corresponding author at: College of Resources and Environmental Sciences, National Academy of Agriculture Green Development, Key Laboratory of Plant-Soil Interactions of Ministry of Education, Beijing Key Laboratory of Farmland Soil Pollution Prevention and Remediation, China Agricultural University, Beijing 100193, PR China.
E-mail address: kaiwang_ly@cau.edu.cn (K. Wang).
[1] Jingjing Li and Jinrui Zhang should be considered joint shared first author.

http://dx.doi.org/10.1016/j.scitotenv.2023.162947
Received 6 January 2023; Received in revised form 15 March 2023; Accepted 15 March 2023
Available online 20 March 2023

proportion (32 %) of all MPs, followed by polyethylene terephthalate (12 %) and polyethylene (8 %). This study also found that a significant positive correlation between rainfall volume and MPs deposition rate. In addition, HYSPLIT back-trajectory modelling showed that the farthest source of deposition MPs may have come from Russia.

1. Introduction

Since the 1940s, plastics and their derivatives have been generated in ever increasingly larger quantities, with the overall consumption of plastics now far exceeding that of most other non-plastic artificial materials (Ostle et al., 2019). As of 2017, the cumulative output of plastics in the world exceeded 10 billion tons, of which ca. 600 million tons were recycled, and <10 % the reused (Geyer et al., 2017). Furthermore, 12 % of the plastics were incinerated, with most (approximately 79 %) of the remaining plastic products being discarded into the natural environment where they may enter the soil, atmosphere or transfer into freshwaters and the ocean by surface runoff (Geyer et al., 2017; Rochman et al., 2013). After entering the environment, plastic waste decomposes due to a combination of physical, chemical and biological weathering processes, forming smaller plastic particles, which continue to accumulate in the environment (Auta et al., 2017; Peng et al., 2020), and exert a stress on the ecological system (Issac and Kandasubramanian, 2021; Zhang et al., 2022). In 2004, the term microplastics (MPs) was proposed (Thompson et al., 2004), which was defined as plastic particles or fragments with a particle size <5 mm. In the following decade, the distribution of MPs in the oceans has become the focus of frequent environmental investigations. The distribution of MPs in the ocean is mainly dependent on geographical characteristics and the combined effects of ocean currents and wave transport (Desforges et al., 2014). Indeed, contamination by MPs around the planet appears ubiquitous. In addition to the marine environment, MPs have been found in polar glaciers (Aves et al., 2022), the offshore environment (Zhang et al., 2019), freshwater bodies (Han et al., 2020), farmland soils (Huang et al., 2020) as well as the atmosphere (Zhang et al., 2020). Recently, research on MPs in the atmosphere has continued to be carried out worldwide (Zhang et al., 2020). However, few studies have focused on atmospheric MPs compared to MPs in other environmental media (Yang et al., 2021a). MPs in the atmosphere can be transported over long distances within the air mass, extending contributing to the ubiquitous spread of MPs pollution (Klein and Fischer, 2019). Therefore, it is of considerable significance to carry out quantitative research on MPs abundance and fate in the atmosphere.

The synthetic textile industry is likely to be a major source of airborne MPs. Previous studies have shown that the global annual output of synthetic textiles exceeds 60 million tons (Gasperi et al., 2018). There are several processes responsible for the generation of atmospheric MPs from synthetic textiles. During the use, cleaning and drying of synthetic textiles, debris is easily generated by fiber tearing (Napper and Thompson, 2016). In addition, grinding, shredding and cutting in the production of synthetic textiles can also generate fibrous debris (Salvador Cesa et al., 2017). It can also come from water-based paints, adhesives, and plastic particles in electronics. For example, plastic resin powders are used in jet technology to remove rust and paint from machinery, engines and hull surfaces (Zhang and Liu, 2018). Commercial desktop 3D printers use thermoplastics as raw materials, resulting in the release of primary MPs into the environment as aerosols (Stephens et al., 2013). During transportation, the resuspension of road dust and the friction between tyres and the road release MPs into the air (Klein and Fischer, 2019). Also, several plastic products and wastes exposed to the natural environment, such as plastic mulch films (Zhang and Liu, 2018), polytunnel covers (Zhang and Liu, 2018) and plastic coatings (Kroon et al., 2018), can degrade, gradually forming MPs under the combined effects of environmental weathering (Yang et al., 2022), air oxidation (Zhang et al., 2021), ultraviolet radiation (Song et al., 2017), and biodegradation (Shen et al., 2019), and then be transported into the atmosphere.

In 2015, the presence of MPs was first observed in atmospheric dust samples collected in the city of Paris (Dris et al., 2015). Subsequently, MPs were observed in atmospheric dust collected in several urban and remote natural areas. Previous studies showed that most MPs observed in the atmosphere were fibrous, and some were fragmented with a foam-like shape (Cai et al., 2017; Dris et al., 2015; Liu et al., 2019b). The particle size of MPs in the atmosphere is at the micron scale, and mostly <500 μm (Zhang et al., 2020). For example, one study reported that 80 % of MPs in the atmosphere of Beijing had the size distribution of 5–20 μm (Li et al., 2020). In general, greater numbers of atmospheric MPs are associated with smaller particle sizes (Allen et al., 2019; Bergmann et al., 2019). The chemical composition of atmospheric MPs varies, including polyethylene terephthalate (PET), polyethylene (PE), polystyrene (PS), polyvinyl chloride (PVC), polypropylene (PP), polyester (PES), polyacrylonitrile (PAN), polyacrylic acid (PAA) and rayon (RY). Among them, PET, PE, PS, and PP are the most commonly reported in the atmosphere, most likely relating to their density and frequent use as everyday plastic products (Geyer et al., 2017). PE and PP can remain suspended in the atmosphere for long period of time due to their low density (Allen et al., 2019, Hidalgo-Ruz et al., 2012). PET has a high density of 1.37–1.45 g/cm^3 (Hidalgo-Ruz et al., 2012), and is widely used in its polyester fiber and textile production (Kuczenski and Geyer, 2010). The morphology and composition of MPs collected from the atmosphere in different regions worldwide are similar, indicating that the transport of MPs in the atmosphere is widespread (Cai et al., 2017; Dris et al., 2015; Liu et al., 2019b).

Until recently, most atmospheric MPs studies have been conducted in densely populated urban areas (Allen et al., 2019) or very remote areas (Aves et al., 2022). However, fewer studies have been conducted in rural areas. A study by Klein and Fischer (2019) showed that the average MPs deposition flux of three rural sampling sites in the Hamburg Hills was 331 particles/m^2/day in the beech/oak forest, 512 particles/m^2/day in the Douglas fir forest and 343 particles/m^2/day in the open field. A recent study by Liao et al. (2021) reported that MPs deposition in the rural area of Wenzhou City in eastern China was 101 particles/m^2/day. In addition to clothing and synthetic textiles, agricultural sources can contribute significantly to atmospheric MPs, e.g. MPs from plastic films, which have been used more and more widely since the 1950s (Kasirajan and Ngouajio, 2012). In China, the annual use of agricultural plastic films between 2011 and 2020 was 2.3–2.6 million tons (National Bureau of Statistics of China, 2021). Since the thickness of polyethylene plastic film used in China is often very thin (4–8 μm), it is difficult to remove it intact from the soil for recycling (Yan et al., 2014). Exposure to UV irradiation accelerates the degradation of plastic film (Yang et al., 2022) and increases the risk of transfer of MPs in the atmosphere following soil disturbance and wind blow. Therefore, it is important to understand the magnitude of atmospheric deposition of MPs in these rural areas.

In this study, samples of MPs in bulk atmospheric deposition were collected on a rainfall event basis from August 2020 to August 2021 at a rural long-term measurement station in Quzhou County, a typical agricultural county in the North China Plain (NCP). The number and size of MPs were measured using fluorescence microscopy, while their chemical composition was detected using micro-Fourier transform infrared (μ-FTIR) spectroscopy. This study provides an overview of the atmospheric MPs pollution situation in a rural region in the NCP and enhances our understanding of MPs as an emerging pollutant in the atmosphere.

2. Materials and methods

2.1. Study area

The experimental site was located in the Quzhou Experiment Station (36°78′01″N, 114°94′51″E, 40 m above sea level) belonging to China Agricultural University (CAU) in Quzhou County, Hebei Province, China (see Fig. 1). There was no vegetation (e.g. trees) around the sampling site, and the passive sampling device was completely exposed to the air. Quzhou County is a typical agricultural county in the North China Plain (NCP). This region has a

temperate semi-humid monsoon climate. It is cold and dry in winter and spring, while it is warm and rainy in summer. The average annual temperature is 13.2 °C, and the average annual rainfall is ca. 490 mm. Nearly 68 % of the rainfall events happen between June and September (Sha, 2021).

2.2. Sampling process

Samples of MPs in the atmospheric bulk deposition were collected using a passive sampler. The sampling period was from August 2020 to August 2021, covering four seasons (i.e. spring - March, April and May; summer - June, July, and August; autumn - September, October, and November; and winter - December, January, and February). The customized stainless steel deposition sampler was installed 100 cm above the ground level, and comprised a 30 cm diameter stainless-steel funnel, a narrow-necked glass bottle, and a metal base. During the sampling period of an entire year, the bulk samples (i.e. the mix of wet and dry atmospheric deposition) were collected in via a modified rainfall sampler. The volume of bulk deposition samples was measured immediately after each rainfall event, and all of the rainwater samples were transferred to aluminum bottles. Both the glass bottles and stainless-steel funnels were rinsed with deionized water three times to ensure that all MPs were collected. In total, 35 atmospheric deposition samples were collected. Details of local rainfall recorded at the sampling site along with the normalized MPs counts per day are provided in Table S1 in Supporting Information (SI). The samples were kept at room temperature until analysis.

2.3. Laboratory analysis

All the samples were filtered onto glass-fiber filters (50 mm in diameter with 0.45 μm in pore size, Shanghai Xingya Co., Ltd., China). To eliminate any organic matter in the samples, the MPs and organic matter on the filter were rinsed into a glass tube with 30 % H_2O_2 solution, and digested in a water bath at 55 °C for 7 days (Allen et al., 2019). The digestion solution was then filtered onto a 0.45 μm glass fiber filter using a vacuum pump. The filter samples were stored in glass Petri-dishes in the dark at room temperature. Each filter was dyed with a Nile Red solution (500 mg/L in methanol) for 10 min (Maes et al., 2017; Meyers et al., 2022; Prata et al., 2019). To remove excess dye, the filter was thoroughly rinsed three times with deionized water. The filters were stored in glass dishes at room temperature, and inspected with a fluorescence microscope within 24 h.

2.4. Fluorescence microscopy

The Nile Red-stained filters containing MPs were initially inspected with a fluorescence microscope (Olympus BX53, Japan). Due to the small size of MPs and the difficulties in quantifying MPs on the whole filter, 10 fields of view (each of 4.4 mm × 3.3 mm) were selected on the filter to calculate the MPs (Qi, 2021). In order to ensure that the selected fields were evenly distributed, the 10 fields of view were selected according to a "Z" shape on each filter. It should be noted that some uncertainty may exist due to selection of 10 fields (accounting for 12 % of the whole membrane) on one filter for measurement instead of the whole filter. The selected fields were observed and photographed in bright field and blue fluorescence, respectively. MPs appeared bright green under the microscope after being dyed with Nile Red (see Fig. 2). The photos observed from the fluorescence microscope were then imported into ImageJ software (https://imagej.nih.gov/ij/) for analysis to obtain the size and number of MPs. Since the detection limit of size of the ImageJ software is 3.23 μm, MPs with a size smaller than 3.23 μm were not capable of being detected in the current study. Therefore, the definition of MPs was operationally defined as being 3.23 μm to 5 mm in our study. More micrographs and fluorescence micrographs of MPs with different morphologies are shown in Table S2.

2.5. Polymer composition

μ-FTIR (Bruker Alpha II FTIR, Germany) was used to determine the chemical composition of potential MPs. The samples of atmospheric MPs were divided into four groups (i.e. spring, summer, autumn and winter samples) according to the sampling season, and 10–24 particles were randomly selected in each season sample for chemical composition identification. A total number of 60 MPs were collected from the filters. A brand-new filter was used as the background (64 scans). The resulting spectra were compared to a spectral library (OPUS) for chemical identification. OPUS is the leading spectroscopy software for state-of-the-art measurement, processing and evaluation of infrared, near-infrared and Raman spectra (Primpke et al., 2017).

2.6. Calculation of MPs deposition rate

Atmospheric deposition is an important source of MPs in land and water environment (Obbard, 2018; Zhang et al., 2016). Estimating the deposition flux of atmospheric MPs is the most intuitive way to understand the

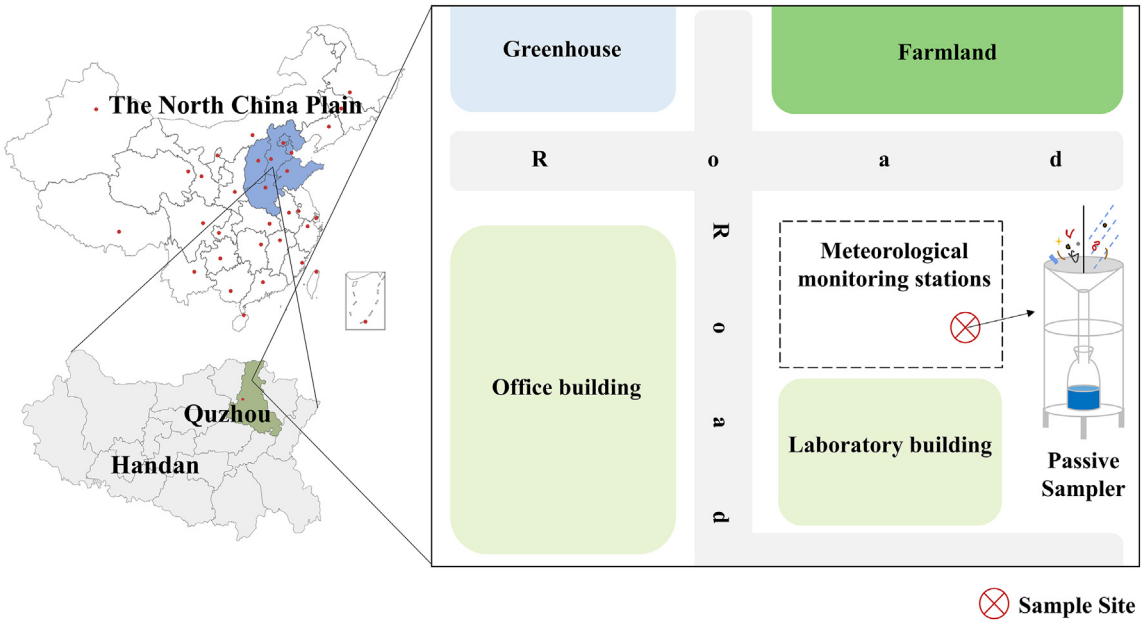

Fig. 1. The location of the rural sampling site in the Quzhou Environmental Monitoring Central Station, Quzhou County in the south of Hebei Province, China and the description of the passive sampling device.

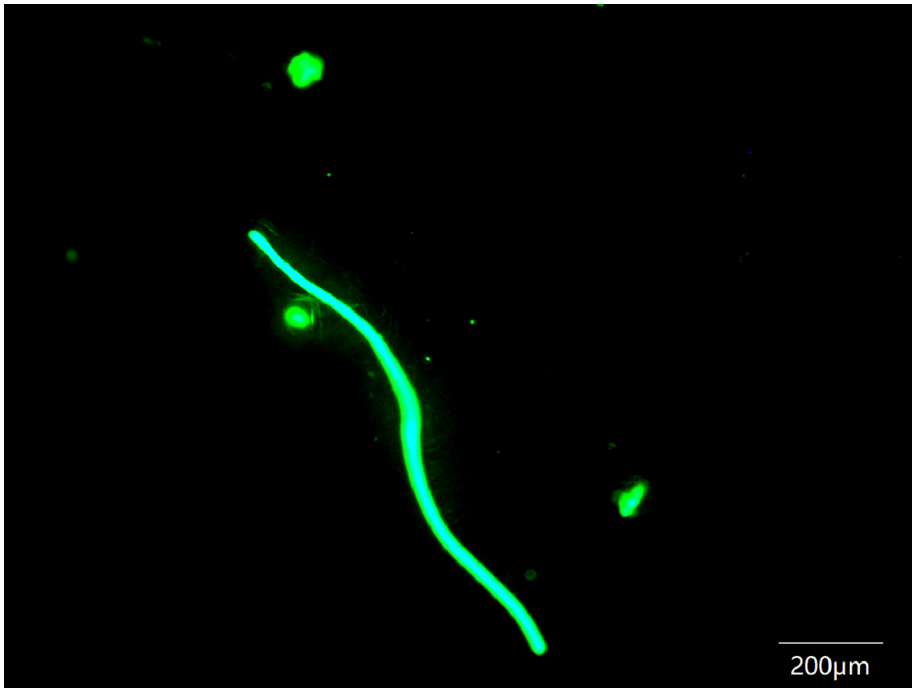

Fig. 2. Example of fluorescence microscopy images of MPs in a rainfall sample under blue fluorescence illumination.

deposition of atmospheric MPs. The earliest calculation method of atmospheric MPs deposition flux was proposed by Zhou et al. (2017). We therefore adopted this method and formula to calculate the deposition rate of atmospheric MPs (*N*) as follows:

$$N = \frac{A_f \times \mathrm{n}}{A_v \times \mathrm{s} \times \mathrm{t}}$$

where, A_f is the effective filtration area of each filter, 12.56 cm^2; A_v is the actual area of each field of view for measurement, 0.1452 cm^2; *n* is the average of particle numbers observed in the 10 fields of view per filter in the microscope (particles); *s* is the area of collection port in the sampling device, 0.071 m^2; *t* is the collection time (day); The MPs deposition rate was calculated by dividing the total number of particles collected in each rainfall event by the number of days between successive sampling dates and as number of particles/m^2/day.

2.7. Statistical analysis

Statistical analysis was accomplished by using SPSS 23.0 and graphing was accomplished by Python 3.7 (64 bit). Regression analysis was applied to test the relationship between rainfall and the MPs abundance. Statistical test was considered significant at *p*-value < 0.05. Simple correlation analysis between the MPs counts and precipitation data was completed using SPSS 26.0 software and standard significance (*P* value), and Pearson correlation test appropriate to the data was used. Statistical significance and extreme difference were represented with $P < 0.05$ and $P < 0.01$, respectively.

2.8. Background contamination

In order to determine the procedural blank of the total extraction procedure, ten laboratory blank samples were processed alongside the field samples. The laboratory blank consisted of 500 mL deionized water and presented information about the background contamination in the laboratory during digestion, filtration and staining. To avoid MPs contamination in the laboratory, cotton laboratory clothes and nitrile gloves were worn during sample collection, pretreatment and analysis. After sampling, the sample was treated on a thoroughly cleaned laboratory bench. All equipment used in the processing procedure in this study was rinsed three times with deionized water and covered with tin foil paper after each step (Klein and Fischer, 2019).

2.9. Atmospheric transport modelling

The open-source modelling software of HYSPLIT is usually used to model the back trajectory of air particle movement from the field site during the monitoring periods (Stein et al., 2015). In current study, the HYSPLIT model was used to simulate the source of atmospheric air mass over the sampling site. The model was run in backward mode for the duration that MPs were estimated to be suspended in the air and then speculated the possible source of atmospheric MPs, and established the source-sink relationship. The input of model included the longitude and latitude of the sampling site, the height of the atmospheric boundary layer (ABL) and the atmospheric migration tracing time, but without the information of particle weight and size. Through modelling, we simulated the atmospheric propagation track in the curved region within 48 h before the date of sample collection. Based on the frequency of atmospheric trajectory, we deduced the potential source of atmospheric MPs. Trajectory frequencies calculated for the sampling site in Quzhou County using HYSPLIT over a 48-h period and at 6-hourly intervals for all sampling dates are provided in Table S4 in SI.

3. Results

3.1. Background contamination

The blank samples contained 4.5 ± 1.7 MPs per view under the fluorescence microscope and the majority of MPs had a fragmented form. The results of all samples were blank-corrected.

3.2. MPs deposition rate

Thirty-five samples of atmospheric bulk deposition were collected in the rural region of Quzhou County, Hebei Province, and the number and chemical composition of MPs were measured for all samples. Numbers of MPs in samples were corrected by deducting the number of MPs measured in the blank samples (which accounted for any contamination caused during sample extraction and the detection process, as well as airborne MPs in the laboratory). As shown in Fig. 3, the MPs deposition rate varied from 86 to 75,421 particles/m^2/day, which were 735–9428, 892–75,421, 280–4244 and 86–1347 particles/m^2/day in spring, summer, autumn and winter, respectively. The atmospheric MPs deposition characteristics were

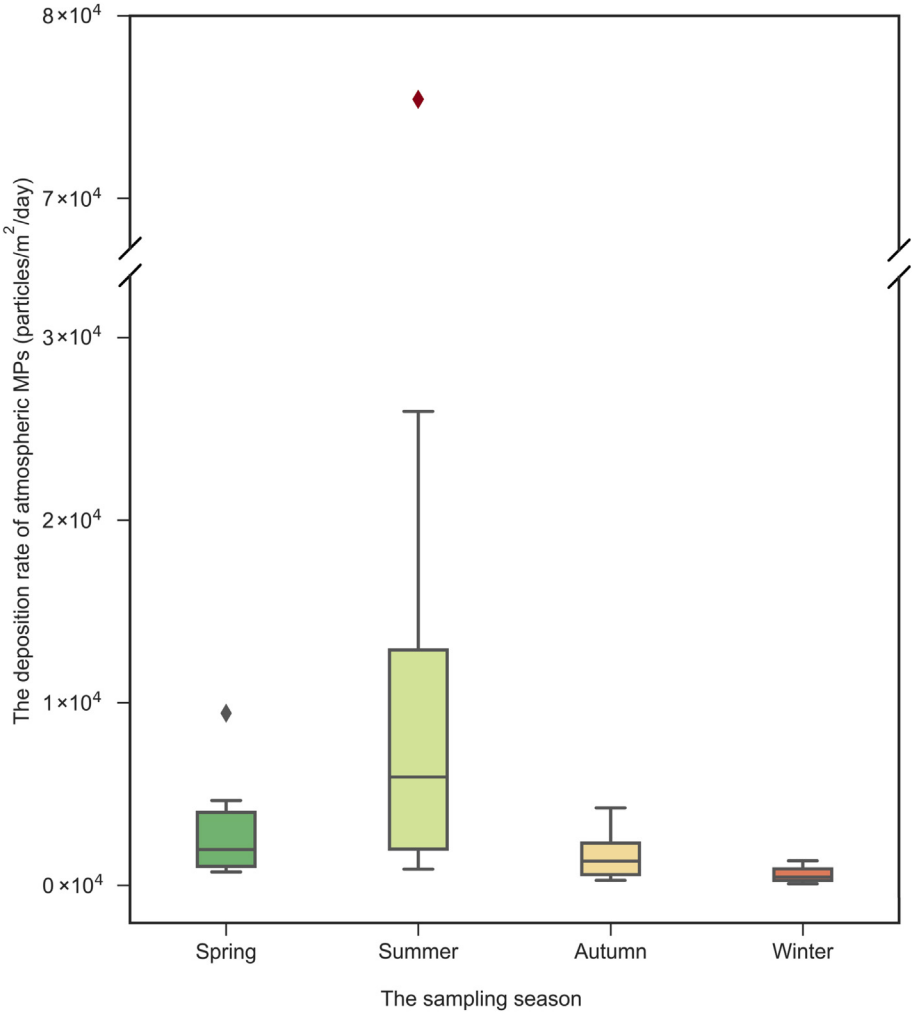

Fig. 3. The average deposition rate of atmospheric MPs for each rainfall event in the rural region of Quzhou County during four seasons from August 2020 to August 2021. There were 35 rainfall events throughout the year, including 7 in spring (March, April and May), 19 in summer (June, July, and August), 6 in autumn (September, October, and November) and 3 in winter (December, January, and February). It should be noted that the dark red point in summer is markedly higher than the other values.

quite different in summer and winter. The MPs deposition rate was greatest and highly variable in summer, while it was lowest in winter with a maximum of only 1347 particles/m^2/day. A total of 20 rainfall events occurred in summer, thus, 20 atmospheric bulk deposition samples were collected and analyzed in the summer season. Only 3 snowfall events occurred in the winter of 2020, resulting in the low MPs deposition rate in winter. The atmospheric MPs deposition rate in spring and autumn was at an intermediate level in the whole year, while the deposition rate in spring was slightly higher than that in autumn.

3.3. Size distribution of MPs

The collected MPs were divided into 6 different particle size classes, and the size distribution of MPs in the atmospheric bulk deposition samples collected from August 19, 2020 to August 19, 2021 are shown in Fig. 4. The finer MPs with the size between 10 and 50 μm accounted for the largest proportion in all samples, i.e. 44.3 % in spring, 48.9 % in summer, 46.5 % in autumn and 37.9 % in winter, respectively. MPs with the size 3.23 μm–10 μm had the second largest proportion, accounting for 31.4 % in spring, 29.5 % in summer, 26.9 % in autumn and 28.2 % in winter. The sizes of MPs ranged from 3.23 to 2645 μm, with a mean value of 43.1 μm. In all samples, larger MPs accounted for a relatively small proportion, among which large MPs with size >500 μm accounted for 0.68 % in all samples, and the largest MPs in all samples had a size of 2645 μm. Overall, the number of MPs samples increased with the decrease of size.

3.4. Chemical composition

Fig. 5 shows the distribution of MPs collected in the rural region of Quzhou County, in the NCP. Since the sampling period was divided by season, the MPs deposition patterns were explored in four seasons: spring (n = 14), summer (n = 22), autumn (n = 16) and winter (n = 8). We randomly screened the collected MPs, and a total number of 60 MPs were examined with μ-FTIR. As shown in Fig. 5, 10 chemical components of MPs were identified, including PE, PP, PS, PVC, PET, Polyamide (PA), Polyurethane (PU), Polyetherimide (PEI) and RY. More types of MPs (8 polymer types) were observed in the summer samples compared to 4 chemical components in spring and winter samples. The MPs were mostly composed of RY, PET and PE in all season samples. The highest proportion of MPs collected in summer samples was PET, accounting for 23 %, while it was RY in spring and autumn samples, accounting for 57 % and 38 % respectively. PE and PET are common packaging materials (Geyer et al., 2017). RY is a form of chemical fiber made from natural polymers through chemical treatment and mechanical processing, and is one of the common textile materials.

3.5. Atmospheric deposition and transport of MPs

HYSPLIT (developed by National Oceanic and Atmospheric Administration, the USA) has been used widely in previous studies for source tracking of persistent organic pollutants (POPs) and suspended particulate matter

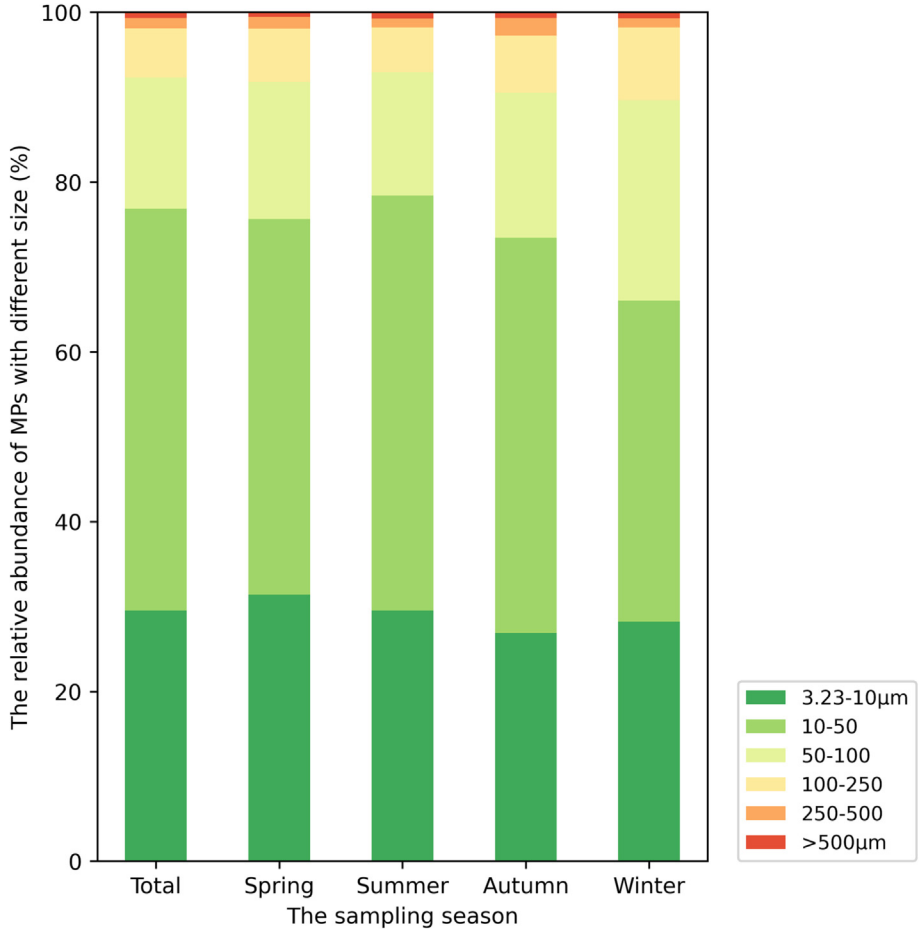

Fig. 4. The relative abundance of atmospheric MPs in each season samples and aggregated samples in terms of particle size. Different colors indicate different sizes of MPs.

(Allen et al., 2019; Stein et al., 2015). Examples of February 24, 2021 trajectory frequencies at Quzhou County, calculated by HYSPLIT for 48-h periods and 6-h intervals with the atmospheric boundary layer (ABL) height of 500 m and 1500 m, respectively, are shown in Fig. 6. HYSPLIT trajectory frequencies with the ABL height of 500 m showed that the probability of MPs collected by Quzhou County from local sources was >90 %, while the possibility of air transport from Shandong Province (east of Quzhou County) and Bohai Bay (northeast of Quzhou) was between 50 % and 90 %. Some of the MPs collected in current study may also come from Mongolia and Russia (>2600 km away), with a probability of 1 %–10 %. In the case of a short duration and high ABL of 1500 m, the frequency distribution of MPs transmission is similar to that with low ABL of 500 m. However, the transmission range of atmospheric particles at ABL height of 1500 m is slightly wider, which showed that the potential source of MPs may also come from the southern region of Quzhou County, such as Anhui and Zhejiang Provinces.

4. Discussion

4.1. Influencing factors of atmospheric MPs deposition

Similar to other particulate matter, the transport and deposition of MPs in the atmosphere is affected by meteorological conditions such as precipitation, wind speed, wind direction, and pollutant concentration (Xia et al., 2020). Local rainfall conditions and MPs deposition rate for each sampling date are provided in Table S1 in SI. In the study carried out in the mountain range of Pyrenees by Allen et al. (2019), precipitation (rainfall and snowfall) showed a positive driving effect on atmospheric MPs deposition. A study conducted in Paris also showed that the lowest deposition fluxes of atmospheric MPs (29 particles/m^2/day) occurred during the dry season and the highest deposition of 280 particles/m^2/day occurred during the rainy season over the sampling period (Dris et al., 2015). In addition, Xia et al. (2020) reported that precipitation events promote the deposition of atmospheric MPs, and the rainfall intensity was positively correlated with the change in the concentration of MPs in the lake before and after rainfall.

As shown in Fig. 7, during the whole sampling period, three heavy rainfall events (68.0, 93.2 and 164.7 mm/day) occurred on August 19, July 20 and July 11, 2021 respectively. We classified rainfall of 68.0 mm/day and 93.2 mm/day as a rainstorm, and rainfall of 164.7 mm/day as a heavy rainstorm (Cheng et al., 2020; Dai et al., 2007). Generally, samples collected on the dates with the heavy rain events had the highest number of MPs. We found a significant positive relationship between MPs deposition rate and the daily precipitation volume ($r^2 = 0.479$; $p < 0.01$), indicating that rainfall has played a positive role in promoting the deposition of MPs.

4.2. Atmospheric MPs deposition characteristic

The MPs deposition flux of 86–75,421 particles/m^2/day in our study was 1–2 orders of magnitude higher than that in other regions (investigating MPs in the atmospheric bulk deposition), including Paris (29–280 particles/m^2/day) (Dris et al., 2015), London (575–1008 particles/m^2/day) (Wright et al., 2020), Dongguan (175–313 particles/m^2/day) (Cai et al., 2017) and Hamburg (136.5–512 particles/m^2/day) (Klein and Fischer, 2019). This is most probably due to differences in the location of sampling site and the different detection methodology for MPs. The NCP, where the site in our study is located, has a dense population and intensive agricultural production activities (National Bureau of Statistics of China, 2021). In the rural area of Quzhou County, cotton, vegetable, and spring corn are

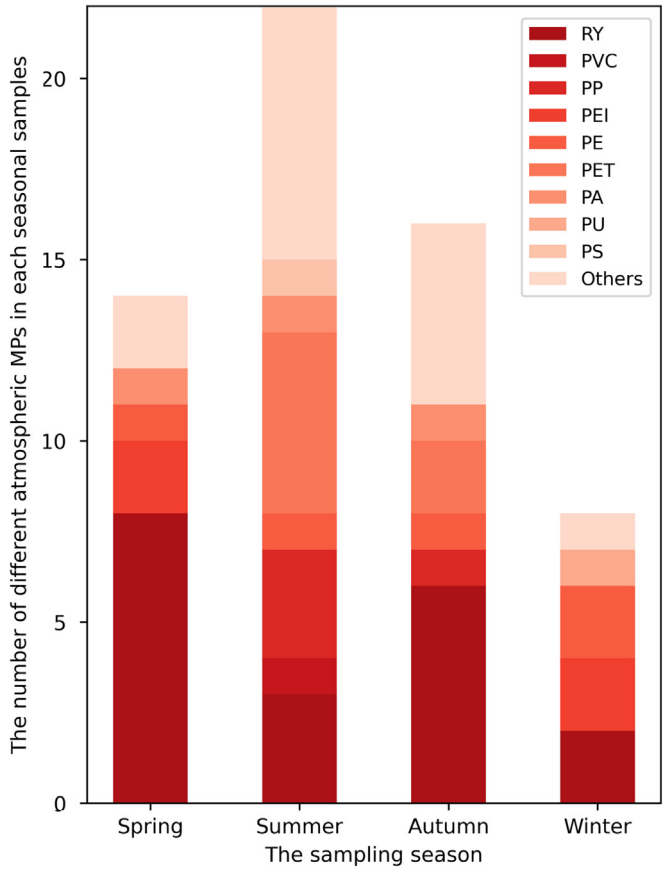

Fig. 5. The number of different types of plastic polymers in atmospheric MPs samples of each season. The detailed percentage value of different chemical composition in each seasonal sample is presented in Table S3 in SI. RY, PVC, PP, PEI, PE, PET, PA, PU and PS refer to Rayon fiber, Polyvinyl chloride, Polypropylene, Polyetherimide, Polyethylene, Polyethylene terephthalate, Polyamide, Polyurethane, Polystyrene, respectively. The "Others" refers to several uncommon plastic materials including phenolic epoxy resin, 2-propenoic acid, acrylonitrile-styrene copolymer.

usually grown through plastic mulch film laid on the soil surface to increase soil temperature and moisture and improve crop yield and quality (Gao et al., 2019; Liu et al., 2019c). Soil disturbance as a result of ploughing and cultivating the soil that has a high plastics content, and wind erosion of agricultural film residue is likely to promote the generation of atmospheric MPs (Jambeck et al., 2015). Climate is also expected to affect airborne MPs abundance. MPs with small size and low density are more easily mobilized and transferred in terrestrial systems through atmospheric transportation and wet/dry deposition (Dehghani et al., 2017). In addition, there are several plastic products processing factories and textile factories distributed near the sampling site (see Fig. S1) that may also have contributed to the higher number of MPs in the atmospheric bulk deposition in our study. According to the average value (7301 particles/m^2/day) of MPs collected in the rural region of the NCP with the land area of around 300,000 km^2, approximately 2190 trillion number of total MPs including around 175 trillion number of PE and 263 trillion number of PET was estimated to deposit daily in the NCP.

The MPs size observed in this study ranged from 3.23 to 2645.37 μm, with an average value of 43.13 μm. A large proportion (77 %) of small-sized (<50 μm) MPs was observed in this study, which is similar to the results of several previous studies. The study of atmospheric MPs in Beijing reported that MPs with small size of 5–20 μm accounted for 80 % of the total MPs (Li et al., 2020). Another study carried out in the Pyrenees found that 85 % of MPs possessed a size smaller than 50 μm (Allen et al., 2019). However, other studies have shown larger MPs sizes, e.g. Dris et al. (2015) suggested that ca. 50 % of the atmospheric MPs in the Paris metropolitan area were >1000 μm in size. The research conducted in Shanghai by Liu et al. (2019a) showed that the average size of MPs was 582.2 μm. Wright et al. (2020) reported that the average sizes of fibrous and non-fibrous MPs in the London metropolitan area were 905 and 164 μm, respectively.

The high abundance and small size of MPs reported in this study may also be attributed to the fluorescent staining method used. In this study, the MPs were stained by Nile Red solution, then photographed using fluorescence microscopy, and information on number and size was identified and counted using ImageJ software. However, visual inspection methods applied in previous studies were more likely to underestimate MPs and result in low MPs counts (Hidalgo-Ruz et al., 2012; Yang et al., 2021b). Therefore, the combination of fluorescence staining, fluorescence microscopy and ImageJ software in our study can detect more smaller sized MPs than other previous studies. The detection limit of MPs size in this study was 3.23 μm, which was much smaller compared to other studies, e.g. 200 μm (Cai et al., 2017) and 100 μm (Dris et al., 2015). Therefore, other studies may underestimate the abundance of small-sized MPs.

The composition of MPs in atmospheric samples has been investigated previously. The main component of fiber in suspended particulate matter in Paris was PP (Dris et al., 2015), while the fiber samples collected from Shanghai were mainly composed of PET (Liu et al., 2019a), and cellulose accounted for 73 % of the MPs in atmospheric deposition in Dongguan city, Guangdong Province (Cai et al., 2017). In this study, RY was the chemical component with the highest proportion of all detected MPs, accounting for 29 %. This may be because there was a large-scale non-woven fabric processing factory (Xin Zhaoyuan Textile CO., Ltd., 36°44′29″N, 114°58′18″E, see Fig. S1) within 15 km of the sampling site, which produced non-woven fabrics for the production of disposable masks (made of RY) during the COVID-19 pandemic period, which may have led to more RY-MP in the sampling dates (Aragaw, 2020; Li et al., 2021). The relatively complex composition of MPs collected in summer compared to spring, autumn and winter may be due to the higher rainfall in summer, when various MPs suspended in the atmosphere are more likely to be washed out. In addition, summer and autumn are also planting or harvesting seasons for corn, wheat, cotton and other crops in Quzhou County, the NCP, and more frequent agricultural activities and soil disturbance can also increase the risk of MPs entering the atmosphere. Furthermore, there is a plastic products factory (Handan Baijiate Toys Co., Ltd., 36°52′14″N, 115°01′27″E, see Fig. S1), located within 1 km of the sampling site, which may contribute to the PP, PE and PVC MPs deposition at the sampling site (Geyer et al., 2017).

As an important carrier of MPs, the atmosphere plays an important role in the long-distance transport of MPs. Due to the small size and light density, MPs can migrate over long distances within the air mass (Zhang et al., 2016). We simulated the long-distance transmission track of atmospheric air mass above the sampling point (Quzhou County, Handan City, the NCP) using the HYSPLIT back-trajectory model. The potential source of atmospheric MPs was investigated according to the atmospheric air mass trajectory, and the source-sink relationship was established. The model showed that the atmospheric MPs in the rural region of Quzhou County, NCP was mainly affected by the local and Shandong Province (east of Quzhou County) air flow with a probability of 90 %, while the probability (1–10 %) of MPs transported from Mongolia and Russia (>2600 km distance) was very low (small probability event). In addition, when the set of ABL height in the model increases, the source range of MPs will be wider. Therefore, longer distance and more accurate atmospheric transport models for atmospheric MPs are necessary.

5. Conclusion

In the current study, we reported the first evidence of the significance of the source of MPs from atmospheric deposition in a rural region of the NCP, China. A large number of MPs were detected in atmospheric bulk deposition collected in the rural site of Quzhou County, in the NCP. The average

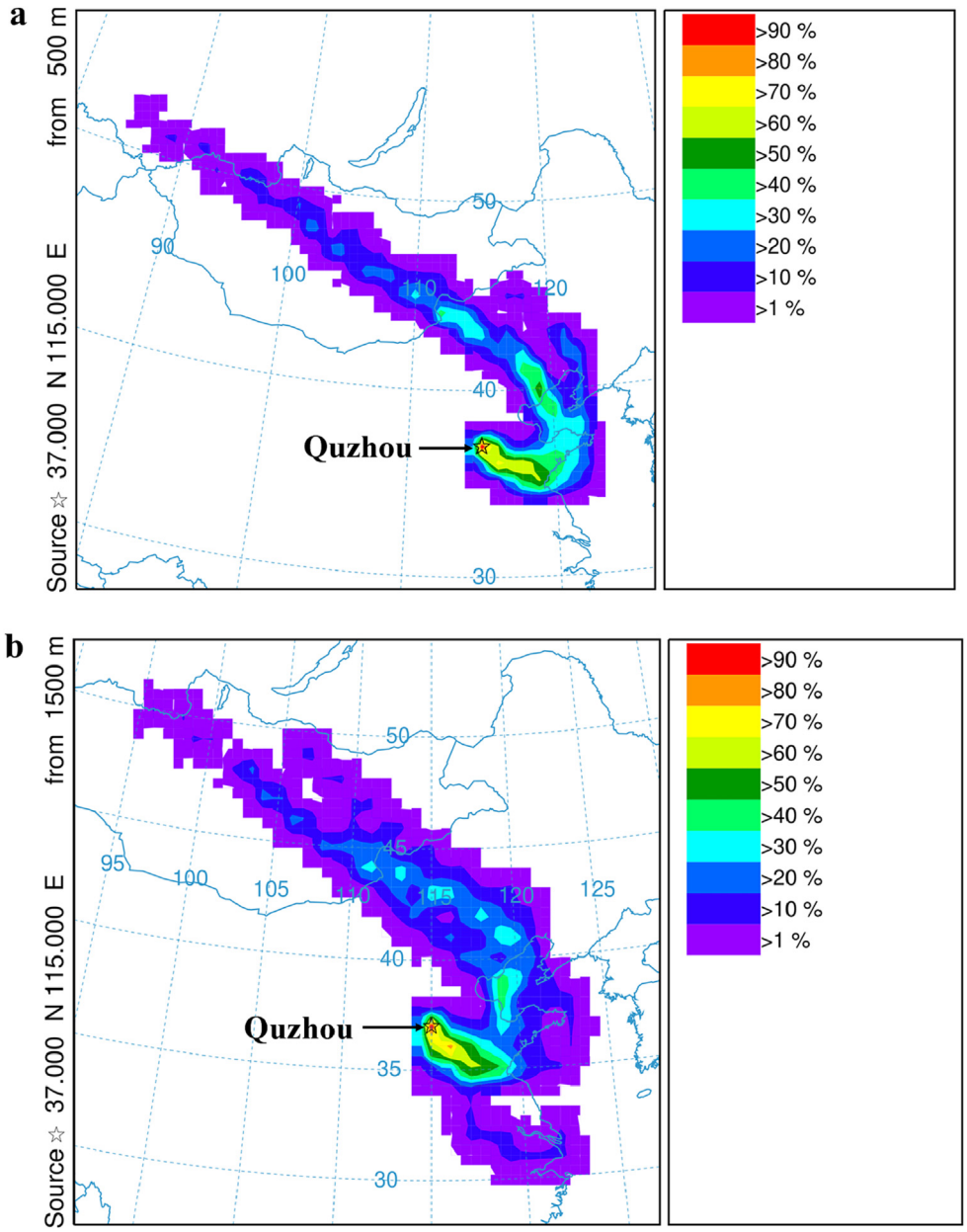

Fig. 6. Trajectory frequencies calculated for Quzhou County using HYSPLIT back-trajectory modelling over a 48-h period at six-hourly intervals for February 24, 2021 with the atmospheric boundary layer (ABL) height of 500 m (a) and 1500 m (b), respectively. The color sequence in the legend represents the possible range of MPs from different regions. The numbers in blue color in the figure represent the latitude and longitude for the region, from Russia to the NCP.

atmospheric MPs deposition rate from August 2020 to August 2021 was 7301 particles/m^2/day, while the highest and lowest atmospheric MPs deposition rate of 11,644 particles/m^2/day and 630 particles/m^2/day were observed in summer and winter, respectively. Smaller sized MPs accounted for a larger proportion of the total number, with 3.23–50 μm of MPs accounting for 77 % of the total MPs. The chemical compositions of atmospheric MPs were dominated by RY, PET and PE. Our study found that rainfall was significantly positively correlated with the atmospheric MPs deposition, indicating that the scouring of rainfall can accelerate the MPs input to the soil. We call for longer distance and more accurate atmospheric transport models that contribute to the understanding of spatial and temporal variability of the deposition characteristics of atmospheric MPs and the factors influencing them. In addition, we recommend that a network of atmospheric MPs deposition samplers is set up across the NCP or globally to further understand the fate of MPs in the atmosphere in local-scale or global-scale.

CRediT authorship contribution statement

Jingjing Li (First author): Sample collection, Sample determination, Data analysis, Writing - original draft, Visualization. **Jinrui Zhang (Co-first author)**: Sample collection, Data analysis, Writing - original draft, Visualization. **Siyang Ren:** Data analysis, Writing – review & editing. **Daqi Huang:** Data analysis. **Fobang Liu:** Writing – review & editing. **Zhen Li:** Sample determination, Data analysis. **Hanyue Zhang:** Writing – review & editing. **Mingyu Zhao:** Writing – review & editing. **Yuxuan Cao:** Writing – review & editing. **Samson Mofolo:** Writing – review & editing. **Jiexi Liang:** Writing – review & editing. **Wen Xu:** Writing – review & editing. **David** L. **Jones:** Writing – review & editing, Funding acquisition. **Dave Chadwick:** Writing – review & editing, Funding acquisition. **Xuejun Liu:** Writing – review & editing, Fund acquisition, Supervision. **Kai Wang:** Writing – original draft, Writing – review & editing, Supervision, Fund acquisition.

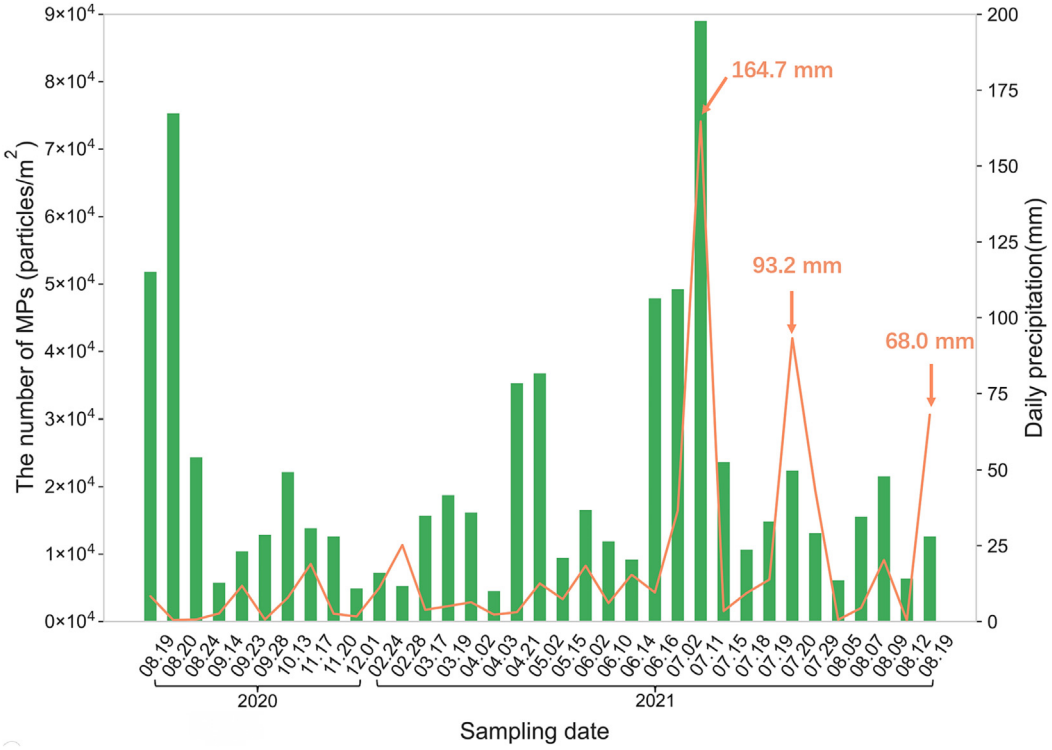

Fig. 7. The pattern of the atmospheric MPs deposition and the daily precipitation in the Quzhou County from August 2020 to August 2021. The green bars represent the MPs deposition, and the orange line represents the daily precipitation for each sampling date.

Data availability

Data will be made available on request.

Declaration of competing interest

All authors have contributed to the work and concur with its submission. All authors declare they have no actual or potential competing financial interests.

Acknowledgments

This research was supported by the National Natural Science Foundation of China under Grant [number 42277097]; the UKRI Global Challenges Research Fund (GCRF) and the Natural Environment Research Council project, "Do agricultural microplastics undermine food security and sustainable development in less economically developed countries?" under Grant [NE/V005871/1], and the High-level Team Project of China Agricultural University.

Appendix A. Supplementary data

Supplementary data to this article can be found online at https://doi.org/10.1016/j.scitotenv.2023.162947.

References

Allen, S., Allen, D., Phoenix, V.R., Le Roux, G., Durántez Jiménez, P., Simonneau, A., Binet, S., Galop, D., 2019. Atmospheric transport and deposition of microplastics in a remote mountain catchment. Nat. Geosci. 12, 339–344. https://doi.org/10.1038/s41561-019-0335-5.

Aragaw, T.A., 2020. Surgical face masks as a potential source for microplastic pollution in the COVID-19 scenario. Mar. Pollut. Bull. 159, 111517. https://doi.org/10.1016/j.marpolbul.2020.111517.

Auta, H.S., Emenike, C.U., Fauziah, S.H., 2017. Distribution and importance of microplastics in the marine environment: a review of the sources, fate, effects, and potential solutions. Environ. Int. 102, 165–176. https://doi.org/10.1016/j.envint.2017.02.013.

Aves, A.R., Revell, L.E., Gaw, S., Ruffell, H., Schuddeboom, A., Wotherspoon, N.E., LaRue, M., McDonald, A.J., 2022. First evidence of microplastics in Antarctic snow. Cryosphere 16, 2127–2145. https://doi.org/10.5194/tc-16-2127-2022.

Bergmann, M., Mutzel, S., Primpke, S., Tekman, M.B., Trachsel, J., Gerdts, G., 2019. White and wonderful? Microplastics prevail in snow from the Alps to the Arctic. Sci. Adv. 5, eaax1157. https://doi.org/10.1126/sciadv.aax1157.

Cai, L., Wang, J., Peng, J., Tan, Z., Zhan, Z., Tan, X., Chen, Q., 2017. Characteristic of microplastics in the atmospheric fallout from Dongguan city, China: preliminary research and first evidence. Environ. Sci. Pollut. Res. Int. 24, 24928–24935. https://doi.org/10.1007/s11356-017-0116-x.

Cheng, Z., Chen, X., Zhang, Y., Jin, L., 2020. Spatio-temporal evolution characteristics of precipitation in the north and south of Qin-ba Mountain area in recent 43 years. Arab. J. Geosci. 13, 848. https://doi.org/10.1007/s12517-020-05860-3.

Dai, A., Lin, X., Hsu, K.-L., 2007. The frequency, intensity, and diurnal cycle of precipitation in surface and satellite observations over low- and mid-latitudes. Clim. Dyn. 29, 727–744. https://doi.org/10.1007/s00382-007-0260-y.

Dehghani, S., Moore, F., Akhbarizadeh, R., 2017. Microplastic pollution in deposited urban dust, Tehran metropolis,Iran. Environ. Sci. Pollut. Res. Int. 24, 20360–20371. https://doi.org/10.1007/s11356-017-9674-1.

Desforges, J.P., Galbraith, M., Dangerfield, N., Ross, P.S., 2014. Widespread distribution of microplastics in subsurface seawater in the NE Pacific Ocean. Mar. Pollut. Bull. 79, 94–99. https://doi.org/10.1016/j.marpolbul.2013.12.035.

Dris, R., Gasperi, J., Rocher, V., Saad, M., Renault, N., Tassin, B., 2015. Microplastic contamination in an urban area: a case study in Greater Paris. Environ. Chem. 12, 592. https://doi.org/10.1071/en14167.

Gao, H., Yan, C., Liu, Q., Ding, W., Chen, B., Li, Z., 2019. Effects of plastic mulching and plastic residue on agricultural production: a meta-analysis. Sci. Total Environ. 651, 484–492. https://doi.org/10.1016/j.scitotenv.2018.09.105.

Gasperi, J., Wright, S.L., Dris, R., Collard, F., Mandin, C., Guerrouache, M., Langlois, V., Kelly, F.J., Tassin, B., 2018. Microplastics in air: are we breathing it in? Curr. Opin. Environ. Sci. Health 1, 1–5. https://doi.org/10.1016/j.coesh.2017.10.002.

Geyer, R., Jambeck, J.R., Law, K.L., 2017. Production, use, and fate of all plastics ever made. Sci. Adv. 3, e1700782. https://doi.org/10.1126/sciadv.1700782.

Han, M., Niu, X., Tang, M., Zhang, B.T., Wang, G., Yue, W., Kong, X., Zhu, J., 2020. Distribution of microplastics in surface water of the lower Yellow River near estuary. Sci. Total Environ. 707, 135601. https://doi.org/10.1016/j.scitotenv.2019.135601.

Hidalgo-Ruz, V., Gutow, L., Thompson, R.C., Thiel, M., 2012. Microplastics in the marine environment: a review of the methods used for identification and quantification. Environ. Sci. Technol. 46, 3060–3075. https://doi.org/10.1021/es2031505.

Huang, Y., Liu, Q., Jia, W., Yan, C., Wang, J., 2020. Agricultural plastic mulching as a source of microplastics in the terrestrial environment. Environ. Pollut. 260, 114096. https://doi.org/10.1016/j.envpol.2020.114096.

Issac, M.N., Kandasubramanian, B., 2021. Effect of microplastics in water and aquatic systems. Environ. Sci. Pollut. Res. 28, 19544–19562. https://doi.org/10.1007/s11356-021-13184-2.

Jambeck, J.R., Geyer, R., Wilcox, C., Siegler, T.R., Perryman, M., Andrady, A., Narayan, R., Law, K.L., 2015. Plastic waste inputs from land into the ocean. Science 347, 768–771. https://doi.org/10.1126/science.126035.

Kasirajan, S., Ngouajio, M., 2012. Polyethylene and biodegradable mulches for agricultural applications: a review. Agron. Sustain. Dev. 32, 501–529. https://doi.org/10.1007/s13593-011-0068-3.

Klein, M., Fischer, E.K., 2019. Microplastic abundance in atmospheric deposition within the Metropolitan area of Hamburg,Germany. Sci. Total Environ. 685, 96–103. https://doi.org/10.1016/j.scitotenv.2019.05.405.

Kroon, F., Motti, C., Talbot, S., Sobral, P., Puotinen, M., 2018. A workflow for improving estimates of microplastic contamination in marine waters: a case study from North-Western Australia. Environ. Pollut. 238, 26–38. https://doi.org/10.1016/j.envpol.2018.03.010.

Kuczenski, B., Geyer, R., 2010. Material flow analysis of polyethylene terephthalate in the US, 1996–2007. Resour. Conserv. Recycl. 54, 1161–1169. https://doi.org/10.1016/j.resconrec.2010.03.013.

Li, Y., Shao, L., Wang, W., Zhang, M., Feng, X., Li, W., Zhang, D., 2020. Airborne fiber particles: types, size and concentration observed in Beijing. Sci. Total Environ. 705, 135967. https://doi.org/10.1016/j.scitotenv.2019.135967.

Li, L., Zhao, X., Li, Z., Song, K., 2021. COVID-19: performance study of microplastic inhalation risk posed by wearing masks. J. Hazard. Mater. 411, 124955. https://doi.org/10.1016/j.jhazmat.2020.124955.

Liao, Z., Ji, X., Ma, Y., Lv, B., Huang, W., Zhu, X., Fang, M., Wang, Q., Wang, X., Dahlgren, R., Shang, X., 2021. Airborne microplastics in indoor and outdoor environments of a coastal city in Eastern China. J. Hazard. Mater. 417, 126007. https://doi.org/10.1016/j.jhazmat.2021.126007.

Liu, K., Wang, X., Fang, T., Xu, P., Zhu, L., Li, D., 2019a. Source and potential risk assessment of suspended atmospheric microplastics in Shanghai. Sci. Total Environ. 675, 462–471. https://doi.org/10.1016/j.scitotenv.2019.04.110.

Liu, K., Wu, T., Wang, X., Song, Z., Zong, C., Wei, N., Li, D., 2019b. Consistent transport of terrestrial microplastics to the ocean through atmosphere. Environ. Sci. Technol. 53, 10612–10619. https://doi.org/10.1021/acs.est.9b03427.

Liu, X., Dong, W., Si, P., Zhang, Z., Chen, B., Yan, C., Zhang, Y., Liu, E., 2019c. Linkage between soil organic carbon and the utilization of soil microbial carbon under plastic film mulching in a semi-arid agroecosystem in China. Arch. Agron. Soil Sci. 65, 1788–1801. https://doi.org/10.1080/03650340.2019.1578346.

Maes, T., Jessop, R., Wellner, N., Haupt, K., Mayes, A.G., 2017. A rapid-screening approach to detect and quantify microplastics based on fluorescent tagging with Nile Red. Sci. Rep. 7. https://doi.org/10.1038/srep44501.

Meyers, N., Catarino, A., Declercq, A., Brenan, A., Devriese, L., Vandegehuchte, M., De Witte, B., Janssen, C., Everaert, G., 2022. Microplastic detection and identification by Nile red staining: towards a semi-automated, cost- and time-effective technique. Sci. Total Environ. 823, 153441. https://doi.org/10.1016/j.scitotenv.2022.153441.

Napper, I.E., Thompson, R.C., 2016. Release of synthetic microplastic plastic fibres from domestic washing machines: effects of fabric type and washing conditions. Mar. Pollut. Bull. 112, 39–45. https://doi.org/10.1016/j.marpolbul.2016.09.025.

National Bureau of Statistics of China, 2021. China Agriculture Yearbook—2021. China Agriculture Press, Beijing (in Chinese).

Obbard, R.W., 2018. Microplastics in Polar Regions: the role of long range transport. Curr. Opin. Environ. Sci. Health 1, 24–29. https://doi.org/10.1016/j.coesh.2017.10.004.

Ostle, C., Thompson, R.C., Broughton, D., Gregory, L., Wootton, M., Johns, D.G., 2019. The rise in ocean plastics evidenced from a 60-year time series. Nat. Commun. 10, 1622. https://doi.org/10.1038/s41467-019-09506-1.

Peng, L., Fu, D., Qi, H., Lan, C.Q., Yu, H., Ge, C., 2020. Micro- and nano-plastics in marine environment: source, distribution and threats - a review. Sci. Total Environ. 698, 134254. https://doi.org/10.1016/j.scitotenv.2019.134254.

Prata, J.C., Reis, V., Matos, J.T.V., da Costa, J.P., Duarte, A.C., Rocha-Santos, T., 2019. A new approach for routine quantification of microplastics using Nile Red and automated software (MP-VAT). Sci. Total Environ. 690, 1277–1283. https://doi.org/10.1016/j.scitotenv.2019.07.060.

Primpke, S., Lorenz, C., Rascher-Friesenhausen, R., Gerdts, G., 2017. An automated approach for microplastics analysis using focal plane array (FPA) FTIR microscopy and image analysis. Anal. Methods 9, 1499–1511. https://doi.org/10.1039/c6ay02476a.

Qi, R., 2021. Characteristics And Ecological Effects of Soil Micro-plastics in Typical Film-covered Agricultural Areas in China. Chinese Academy of Agricultural Sciences PhD.

Rochman, C.M., Browne, M.A., Halpern, B.S., Hentschel, B.T., Hoh, E., Karapanagioti, H.K., Ríos-Mendoza, L.M., Takada, H., Teh, S.J., Thompson, R.C., 2013. Policy: classify plastic waste as hazardous. Nature 494, 169–171. https://doi.org/10.1038/494169a.

Salvador Cesa, F., Turra, A., Baruque-Ramos, J., 2017. Synthetic fibers as microplastics in the marine environment: a review from textile perspective with a focus on domestic washings. Sci. Total Environ. 598, 1116–1129. https://doi.org/10.1016/j.scitotenv.2017.04.172.

Sha, Z., 2021. Potential of NH3 Mitigation And Effect of Stable Fertilizers on Conservation And Loss Control in Croplands. China Agricultural University PhD.

Shen, M., Zhang, Y., Zhu, Y., Song, B., Zeng, G., Hu, D., Wen, X., Ren, X., 2019. Recent advances in toxicological research of nanoplastics in the environment: a review. Environ. Pollut. 252, 511–521. https://doi.org/10.1016/j.envpol.2019.05.102.

Song, Y.K., Hong, S.H., Jang, M., Han, G.M., Jung, S.W., Shim, W.J., 2017. Combined effects of UV exposure duration and mechanical abrasion on microplastic fragmentation by polymer type. Environ. Sci. Technol. 51, 4368–4376. https://doi.org/10.1021/acs.est.6b06155.

Stein, A.F., Draxler, R.R., Rolph, G.D., Stunder, B.J.B., Cohen, M.D., Ngan, F., 2015. NOAA's HYSPLIT atmospheric transport and dispersion modeling system. Bull. Am. Meteorol. Soc. 96, 2059–2077. https://doi.org/10.1175/BAMS-D-14-00110.1.

Stephens, B., Azimi, P., El Orch, Z., Ramos, T., 2013. Ultrafine particle emissions from desktop 3D printers. Atmos.Environ. 79, 334–339. https://doi.org/10.1016/j.atmosenv.2013.06.050.

Thompson, R.C., Olsen, Y., Mitchell, R.P., Davis, A., Rowland, S.J., John, A.W., McGonigle, D., Russell, A.E., 2004. Lost at sea: where is all the plastic? Science 304, 838. https://doi.org/10.1126/science.1094559.

Wright, S.L., Ulke, J., Font, A., Chan, K.L.A., Kelly, F.J., 2020. Atmospheric microplastic deposition in an urban environment and an evaluation of transport. Environ. Int. 136, 105411. https://doi.org/10.1016/j.envint.2019.105411.

Xia, W., Rao, Q., Deng, X., Chen, J., Xie, P., 2020. Rainfall is a significant environmental factor of microplastic pollution in inland waters. Sci. Total Environ. 732, 139065. https://doi.org/10.1016/j.scitotenv.2020.139065.

Yan, C., He, W., Turner, N.C., Liu, E., Liu, Q., Liu, S., 2014. Plastic-film mulch in Chinese agriculture: importance and problems. World Agric. 4 (2), 32–36.

Yang, L., Zhang, Y., Kang, S., Wang, Z., Wu, C., 2021a. Microplastics in soil: a review on methods, occurrence, sources, and potential risk. Sci. Total Environ. 780, 146546. https://doi.org/10.1016/j.scitotenv.2021.146546.

Yang, L., Zhang, Y., Kang, S., Wang, Z., Wu, C., 2021b. Microplastics in soil: a review on methods, occurrence, sources, and potential risk. Sci. Total Environ. 780, 146546. https://doi.org/10.1016/j.scitotenv.2021.146546.

Yang, Z., Lu, F., Zhang, H., Wang, W., Xu, X., Shao, L., Che, Z., Lu, B., Ye, J., He, P., 2022. A neglected transport of plastic debris to cities from farmland in remote arid regions. Sci. Total Environ. 807, 150982. https://doi.org/10.1016/j.scitotenv.2021.150982.

Zhang, G.S., Liu, Y.F., 2018. The distribution of microplastics in soil aggregate fractions in southwestern China. Sci. Total Environ. 642, 12–20. https://doi.org/10.1016/j.scitotenv.2018.06.004.

Zhang, K., Su, J., Xiong, X., Wu, X., Wu, C., Liu, J.-t., 2016. Microplastic pollution of lakeshore sediments from remote lakes in Tibet plateau,China. Environ. Pollut. 219, 450–455. https://doi.org/10.1016/j.envpol.2016.05.048.

Zhang, C., Zhou, H., Cui, Y., Wang, C., Li, Y., Zhang, D., 2019. Microplastics in offshore sediment in the Yellow Sea and East China Sea,China. Environ. Pollut. 244, 827–833. https://doi.org/10.1016/j.envpol.2018.10.102.

Zhang, Y., Kang, S., Allen, S., Allen, D., Gao, T., Sillanpää, M., 2020. Atmospheric microplastics: a review on current status and perspectives. Earth Sci. Rev. 203, 103118. https://doi.org/10.1016/j.earscirev.2020.103118.

Zhang, K., Hamidian, A.H., Tubic, A., Zhang, Y., Fang, J.K.H., Wu, C., Lam, P.K.S., 2021. Understanding plastic degradation and microplastic formation in the environment: a review. Environ. Pollut. 274, 116554. https://doi.org/10.1016/j.envpol.2021.116554.

Zhang, J., Ren, S., Xu, W., Liang, C., Li, J., Zhang, H., Li, Y., Liu, X., Jones, D.L., Chadwick, D.R., Zhang, F., Wang, K., 2022. Effects of plastic residues and microplastics on soil ecosystems: a global meta-analysis. J. Hazard. Mater. 435, 129065. https://doi.org/10.1016/j.jhazmat.2022.129065.

Zhou, Q., Tian, C., Luo, Y., 2017. Various forms and deposition fluxes of microplastics identified in the coastal urban atmosphere. Chin. Sci. Bull. 62, 3902–3909. https://doi.org/10.1360/n972017-00956.